ISSN 1063-7710, Acoustical Physics, 2016, Vol. 62, No. 1, pp. 38–45. © Pleiades Publishing, Ltd., 2016.
Original Russian Text © A.V. Nikolaeva, S.A. Tsysar, O.A. Sapozhnikov, 2016, published in Akusticheskii Zhurnal, 2016, Vol. 62, No. 1, pp. 29–37.

NONLINEAR ACOUSTICS

Measuring the Radiation Force of Megahertz Ultrasound Acting on a Solid Spherical Scatterer

A. V. Nikolaeva[a], S. A. Tsysar[a], and O. A. Sapozhnikov[a, b]

[a] *Moscow State University, Moscow, 119991 Russia*

[b] *Center for Industrial and Medical Ultrasound, Applied Physics Laboratory-University of Washington, Seattle, WA, 98105 USA*

e-mail: niko200707@mail.ru

Received March 25, 2015

Abstract—The paper considers the problem of precise measurement of the acoustic radiation force of an ultrasonic beam on targets in the form of solid spherical scatterers. Using known analytic relations, a numerical model is developed to perform calculations for different sizes of spherical scatterers and arbitrary frequencies of the incident acoustic wave. A novel method is proposed for measuring the radiation force, which is based on the principle of acoustic echolocation. The radiation force is measured experimentally in a wide range of incident wave intensities using two chosen methods differing in the way the location of the target is controlled.

Keywords: radiation force, wave scattering, acoustic beams

DOI: 10.1134/S1063771016010048

INTRODUCTION

The occurrence of the acoustic radiation force is a nonlinear acoustic effect conditioned by the transfer of wave momentum to absorbing or scattering objects [1–3]. A similar effect is widely known for electromagnetic waves, especially in optics, where it is called light pressure. A visual demonstration of the manifestation of the radiation force of ultrasound is the "acoustic fountain" effect—the phenomenon of a hydrodynamic jet that occurs when an ultrasound beam is focused on the free surface of a fluid [4, 5]. The radiation force also makes it possible to achieve levitation of small particles and microbubbles or to create hydrodynamic flows in a fluid (acoustic streaming) owing to absorption of the ultrasound beam by the fluid [6–9]. The phenomenon of the acoustic radiation force is used quite widely in practice. Thus, this effect is used in modern ultrasound metrology to measure the acoustic power of therapeutic and diagnostic sources [10]. Recently, other applications of the radiation force effect have been developed: an example is ultrasound devices for remote manipulation of human kidney stones [11]. Since the corresponding forces are relatively small, it is very important to develop precise methods for measuring them.

Theoretical models describing the phenomenon of the radiation force nowadays are quite well developed. It is possible to single out the case of particles whose diameters are much smaller than the wavelength. For this, radiation force theory is appreciably simplified [12]. However, in practice, the sizes of scattering objects are frequently comparable to or larger than the wavelength. This work considers precisely this case. For such situations, analytic methods for calculating the size of the radiation force have also been developed [13–17]. In addition, the effects have been described and expressions obtained for finding the force when calculating the viscosity of the surrounding fluid [18].

In addition to analytic models, differing numerical methods have also been developed to calculate the radiation force. Many authors have succeeded in determining the force, which with good accuracy agrees with theoretically obtained data. Thus, the well-developed mathematical apparatus opens up great possibilities for the practical application of this phenomenon, for which of undoubted importance is the problem of conducting precise measurements of the magnitude of the radiation force. The authors of [19] described one of the first experiments on measuring the radiation force exerted by a plane traveling wave. All measurements were performed for the frequency range of 450 kHz–1 MHz. The obtained experimental points coincide within error limits of 3% with the theoretical results obtained in [14] taking into account the elasticity of the scatterer. As a result, different modifications of experimental setups and methods for measuring the force were proposed [20–22], each of which has its own pluses and minuses. However, even though the experiments coincide quite well with the theoretical results, obtaining accurately measured and reliably predicted force values is still problematic. This is the subject of our paper.

In this work, using known analytic relations, a numerical model is developed to calculate the force for

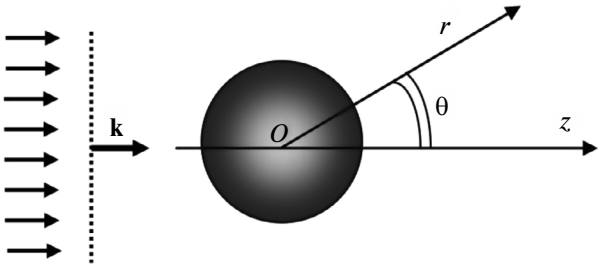

Fig. 1. Geometry of problem of a plane wave scattered by a sphere.

spherical scatterers of different sizes and arbitrary frequencies of the incident acoustic wave. We describe in detail experimental research on measuring the radiation force in a wide range of incident beam intensities using two chosen methods differing in the way the target is controlled. Schemes of experimental setups and methods of measuring the radiation force are presented, as well as obtained experimental data in graph form, and the results are analyzed.

THEORETICAL STUDY OF THE ACOUSTIC RADIATION FORCE

Following [14, 17], let us briefly present the main information on the theoretical model used in this study to find the value of the radiation force acting on an elastic spherical scatterer in a fluid. To determine the radiation force on some obstacle, it is necessary to take into account the change in the wave momentum related to scattering at the wave by this obstacle. Therefore, the calculation algorithm consists of two main stages: first, the problem of sound scattering by a sphere is solved and then the results for calculating the scattered wave are used to calculate the radiation force.

Let us assume that the medium surrounding the scatterer is an ideal fluid with density ρ and sound propagation velocity in it c. Let us place the origin at the center of the considered sphere (Fig. 1).

Consider a plane harmonic wave of frequency $f = \omega/(2\pi)$ falling onto a sphere of radius a, so that the corresponding wavenumber is $k = \omega/c$. In this case, the acoustic pressure $p'(\mathbf{r},t)$ and particle velocity $\mathbf{v}'(\mathbf{r},t)$ are written in the form

$$p' = \frac{P}{2}e^{-i\omega t} + \frac{P^*}{2}e^{i\omega t}, \quad \mathbf{v}' = \frac{\mathbf{V}}{2}e^{-i\omega t} + \frac{\mathbf{V}^*}{2}e^{i\omega t}, \qquad (1)$$

where P and $\mathbf{V}$ are the complex amplitudes of pressure and velocity, respectively. The pressure complex amplitude P is the solution to the Helmholtz equation $\Delta P + k^2 P = 0$. The total acoustic field is the sum of the incident and scattered waves: $P = P_{\text{inc}} + P_{\text{sc}}$, where P, P_{inc}, and P_{sc} are the complex amplitudes of the total, incident, and scattered (by the obstacle) fields, respectively. The expression for the amplitude of the plane wave P_{inc} in spherical coordinates is represented in the form of a series [23]:

$$P_{\text{inc}} = p_0 e^{ikr\cos\theta} = p_0 \sum_{n=0}^{\infty} i^n (2n+1) j_n(kr) P_n(\cos\theta), \quad (2)$$

where r and θ are the spherical coordinates (Fig. 1), $j_n(\varsigma) = \sqrt{\pi/(2\varsigma)}J_{n+1/2}(\varsigma)$ is the spherical Bessel function, and $P_n(\cos\theta)$ is the Legendre polynomial. The scattered field P_{sc} in turn is represented in the form of an expansion [23]:

$$P_{\text{sc}} = p_0 \sum_{n=0}^{\infty} b_n h_n^{(1)}(kr) P_n(\cos\theta), \qquad (3)$$

where $h_n^{(1)}(kr) = j_n(kr) + iy_n(kr)$ is the Hankel function of the first kind; $y_n(\varsigma) = \sqrt{\pi/(2\varsigma)}Y_{n+1/2}(\varsigma)$, $Y_n(\varsigma)$ is the Neumann function. The coefficients b_n characterizing acoustic wave scattering are found from the boundary conditions on the surface of the scatterer. Since the fluid is considered inviscid, these conditions consist in the continuity of the normal velocity and stress components, as well as in the absence of shear stress on the surface of the scatterer. For a solid spherical scatterer with density ρ* and longitudinal c_l and transverse c_t sound propagation velocities in the scatterer material, coefficient b_n taking into account the boundary conditions is written as follows:

$$b_n = -\frac{F_n j_n(ka) - kaj_n'(ka)}{F_n h_n^{(1)}(ka) - kah_n^{(1)'}(ka)}, \qquad (4)$$

where F_n is a function depending on ρ*/ρ, c_l/c, and c_t/c [14]:

$$F_n = \frac{1}{2}\frac{\rho}{\rho^*}x_2^2 \frac{\dfrac{x_1 j_n'(x_1)}{x_1 j_n'(x_1) - j_n(x_1)} - \dfrac{2n(n+1)j_n(x_2)}{(n+2)(n-1)j_n(x_2) + x_2^2 j_n''(x_2)}}{\dfrac{x_1^2[\sigma(1-2\sigma)j_n(x_1) - j_n''(x_1)]}{x_1 j_n'(x_1) - j_n(x_1)} - \dfrac{2n(n+1)[j_n(x_2)x_2 j_n'(x_2)]}{(n+2)(n-1)j_n(x_2) + x_2^2 j_n''(x_2)}}, \qquad (5)$$

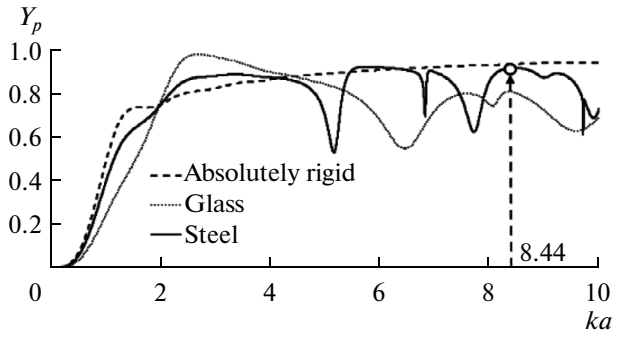

Fig. 2. Dependence of specific radiation force on dimensionless parameter ka for different scatterers. Parameters of immersion fluid: $c = 1500$ m/s, $\rho = 1000$ kg/m^3 (water). Circle on curve for steel sphere corresponds to experiment; here, $ka = 8.44$ and $Y_p = 0.92$.

where ρ is the density of the surrounding fluid, $x_1 = \frac{\omega}{c_l}a$, $x_2 = \frac{\omega}{c_t}a$, σ is the Poisson coefficient for a solid. In the particular case of an absolutely rigid scatterer, $F_n = 0$, which leads to a value of the coefficient for scattering of a plane wave by a rigid sphere of $b_n = -\frac{j_n'(ka)}{h_n^{(1)'}(ka)}$ [23]. The obtained expression for the total field $P = P_{\text{inc}} + P_{\text{sc}}$ for scattering of an acoustic wave by an elastic sphere takes into account excitation of longitudinal and shear waves inside the scatterer,

$$P = p_0\sum_{n=0}^{\infty} i^n(2n+1)\left[j_n(kr) + b_n h_n^{(1)}(kr)\right]P_n(\cos\theta) \quad (6)$$

and makes it possible to calculate the size of the acoustic radiation force acting on the spherical scatterer from the plane wave.

The second stage is direct calculation of the radiation force based on the solved scattering problem. The radiation force is a quadratic quantity of acoustic perturbations; to determine it, it is necessary to take into account quantities of the second order of smallness that do not turn to zero after averaging over time. In the quadratic approximation, the radiation force is written in the form of an integral over a closed surface S containing in itself the studied scatterer [24]:

$$\mathbf{F} = \left\langle \oiint \left[L\mathbf{n} - \rho\mathbf{v}'(\mathbf{v}'\cdot\mathbf{n})\right]dS \right\rangle, \quad (7)$$

where $L = \rho\mathbf{v}'^2/2 - p'^2/(2\rho c^2)$, $\mathbf{n}$ is the vector of the external normal to the element of the surface dS; $\mathbf{v}'$ and p' are, respectively, the particle velocity and acoustic pressure, which are found from the solution to the scattering problem; and angle brackets $\langle . \rangle$ denote averaging over the wave period.

In the case of harmonic wave (1), expression (7) is rewritten via the complex amplitudes of pressure P and velocity $\mathbf{V} = \nabla P/(i\rho\omega)$:

$$\mathbf{F} = \oiint \left[\left(\frac{\rho|\mathbf{V}|^2}{4} - \frac{|P|^2}{4\rho c^2}\right)\mathbf{n} - \frac{\rho}{2}\mathrm{Re}\left[\mathbf{V}^*(\mathbf{V}\cdot\mathbf{n})\right]\right]dS. \quad (8)$$

In the case of a spherical scatterer, the sought radiation force $\mathbf{F}$ acts along the wave propagation axis z and has a single component F_z (in the general case, the radiation force has all three components). The analytic expression for component F_z is presented in [25].

For numerical calculation in Fortran using the above-mentioned formulas, a code was written to determine the radiation force acting on an elastic spherical scatterer in a fluid. The code assigns the parameters of the scatterer, such as density, radius, velocity of longitudinal and shear waves in the scatterer material, as well as the parameters of the surrounding fluid $c = 1500$ m/s and $\rho = 1000$ kg/m^3 (water). During calculations it was considered that the surrounding fluid was ideal; i.e., the viscosity and heat conductivity of the medium were not taken into account. To find the force, expression (8) was used, written for the force component F_z. For numerical calculation of such quantities as the amplitudes of the pressure and particle velocity, summation was performed from 0 to some finite number $N = 3...5\ ka$.

Since the radiation force acting on the scatterer depends on the incident wave intensity, for convenience of analysis in calculations, the dimensionless quantity Y_p is introduced—the specific radiation force, which is defined as

$$Y_p = F_z c/\left(I\pi a^2\right), \quad (9)$$

where I is the incident wave intensity, c is the sound velocity in a fluid, and a is the radius of the scatterer.

The plot in Fig. 2 shows the dependence of the normalized quantity Y_p on dimensionless parameter ka. It shows the dependences for spheres made of different materials, steel and glass, as well as for an absolutely rigid scatterer. The parameters of the materials used in calculations are as follows: steel—velocity of longitudinal waves $c_l = 5240$ m/s, velocity of shear waves $c_t = 2978$ m/s; glass—$c_l = 5570$ m/s, $c_t = 3515$ m/s. Thus, the program makes it possible to calculate the magnitude of the radiation force for spherical scatterers of any radius and density for known parameters of a plane acoustic wave, such as frequency and intensity.

The calculated curves $Y_p = Y_p(ka)$ coincide with the dependences obtained earlier for the same materials by the authors of other works [21, 22]. One can see from the plots that in the case of an absolutely rigid scatterer, with an increase in frequency, the specific radiation force rapidly increases; however, after the frequency attains a value at which the radius of the scatterer becomes on the order of the wavelength, the increase slows and approaches saturation: the quantity Y_p hardly depends at all on the frequency of the incident plane wave. For glass and stainless steel, the pattern is somewhat different. For them, it is possible to distinctly observe local dips of the $Y_p(ka)$ curve, which

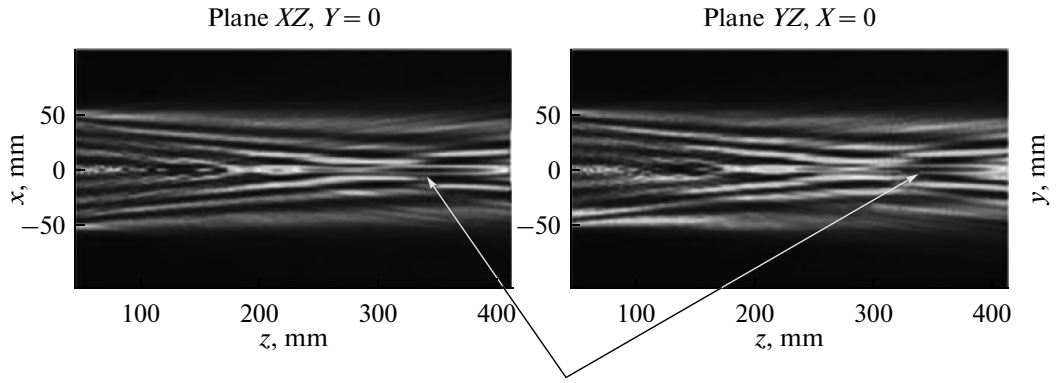

Fig. 3. Two-dimensional patterns of distribution of amplitude of acoustic field pressure of plane source in two planes (x, z), (y, z) for distance z from source of 0 to 400 mm. Arrows indicate region of interest.

correspond to resonance elastic oscillations of the sphere at the corresponding frequencies.

During experiments, the acoustic parameters of the scatterer material can differ somewhat from the tabulated values, which can reflect on the accuracy of theoretically calculating the value of the force in cases when the wave frequency is close to that of any resonance. In order to avoid related errors, it is desirable to choose the wave frequency in a smooth area of the $Y_p(ka)$ curve. This requirement was taken into account when choosing the operating frequency of the source f and the radius a of the steel sphere used as a scatterer in the above-described experiments. Based on the calculated theoretical dependences and taking into account the value of the operating frequency of the source $f = 1.119$ MHz, a steel sphere with a radius of $a = 1.8$ mm was chosen as the target (Fig. 2). Note that the size of the normalized radiation force $Y_p(ka) = 0.92$ in this case is close to its value for an absolutely rigid scatterer.

EXPERIMENTAL MEASUREMENT OF THE RADIATION FORCE ACTING ON A SOLID-STATE ELASTIC SCATTERER

The theoretical model makes it possible to calculate with high accuracy the size of the force acting on a spherical obstacle. However, an important problem, as already mentioned, is the possibility of high-precision measurements of the radiation force. To conduct similar measurements, it is necessary to satisfy several conditions: first, it is necessary to suppress the possible influence of hydrodynamic flows that inevitably arise in intense fields; second, it is necessary to ensure the condition of plane wave incidence on the scatterer.

In the study, hydrodynamic forces are eliminated by introducing a thin sound-transparent film into the experimental setup, directly in front of the scatterer.

The plane wave condition is fulfilled, first, by using a special absorber to eliminate reverberation. Second, the spherical scatterer is placed in a homogeneous, on the scale of the target, region of the field. In order to exactly determine this region of the scatterer, it is necessary to know the distribution of the field pressure amplitude in a wide range of distances from the source. For this, it is possible to use the acoustic holography method [26–28], which measures the amplitude and phase of the pressure along some chosen test surface and calculates the acoustic field at the source by solving the inverse radiation problem using the Rayleigh integral:

$$V(\mathbf{r}) = \frac{i\omega\rho_0}{2\pi}\int P(\mathbf{r}')\frac{e^{-ik|\mathbf{r}-\mathbf{r}'|}}{|\mathbf{r}-\mathbf{r}'|}dS', \qquad (10)$$

where $V(\mathbf{r}), P(\mathbf{r}')$ are the complex amplitudes of the normal component of the particle velocity at the surface of the source and the acoustic pressure on the test plane, respectively; dS' is the element of the integration area along the test surface. Knowing the distribution at the surface of the source, we can easily determine the field of the source at any point in space by solving the direct problem. This very method was used to determine the field of a piezoceramic plane source (operating frequency 1.119 MHz, diameter 100 mm) used in the experiment to determine the radiation force. The procedure of measuring the field is described in detail in [26, 28]. As a result of reconstructing the source field using acoustic holography, the distance used in the experiment was $z = 325$ m on the source axis (Fig. 3). The field in a certain region around this point (on the order of 10 mm in the transverse and 70 mm in the longitudinal direction with respect to the source axis) is homogeneous, which makes it possible to use the assumption about a plane wave.

Yet another important aspect of high-precision measurements is the method of attaching the scatterer in the experimental setup. At the first stages of experimental research, a method proposed in a number of previous works was used—suspension by an inelastic thread [20]. So that the sphere would deviate only along one direction, the thread was suspended and

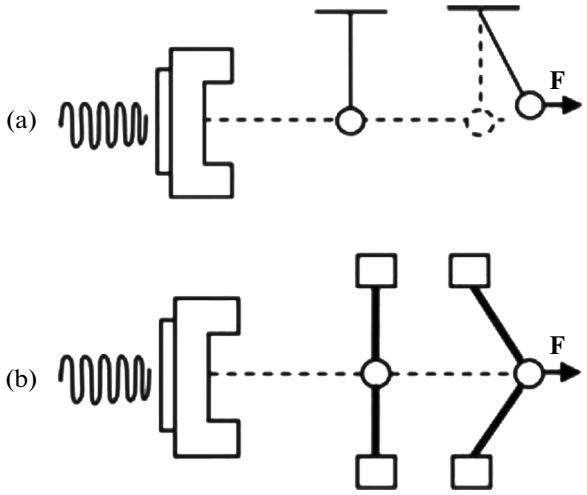

Fig. 4. Methods of fixing scatterer in experimental setup: (a) on inelastic threads, (b) on four elastic threads.

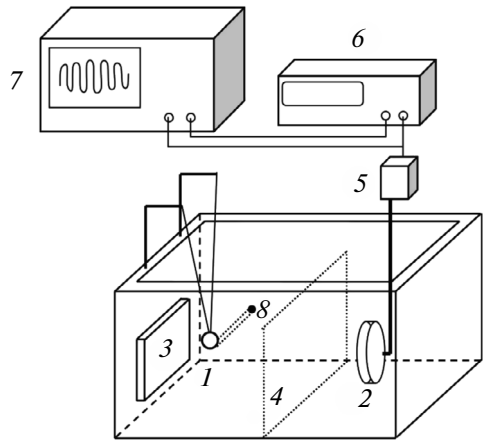

Fig. 5. Scheme of experimental setup with method of measuring displacement of scatterer using laser beam. Elastic steel scatterer *1* with radius $a = 1.8$ mm, acoustic transducer *2* with operating frequency $f = 1.19$ MHz and diameter $d = 10$ cm, acoustic absorber *3*, thin sound-transparent film *4*, signal amplifier *5* with power of 9 W and operating frequency range of 1–5.5 MHz, Agilent 33250A signal generator outputting continuous harmonic signal, oscilloscope *7*, laser beam *8*.

folded in a V-shape. Here, the lower point of the V was fixed to the upper point of the studied sphere.

Such a fixation method is highly sensitive to small displacements of the sphere from a state of equilibrium. However, there is also a drawback. As mentioned above, during experimental research, it is important to know the region of the field in which the scatterer is located. It suffices merely to observe the field if the scatterer during any shift is located on the source axis. The scatterer suspended on fine threads, when deviating from a state of equilibrium, begins to rise with respect to the level of the axis, and the greater the magnitude of the radiation force, the stronger the displacement from the axis (Fig. 4a). Nevertheless, for small axial displacements, the vertical component is small and the effect is weakly pronounced, which makes it possible to conduct measurements. With such an approach, displacement of the scatterer under the action of an acoustic wave is measured with a laser beam (Fig. 5), which makes it possible to calculate the size of the force using a quite simple formula:

$$F_{\text{rad}} = \frac{4}{3}\pi a^3(\rho - \rho_w)g\frac{\Delta x}{l}, \qquad (11)$$

where a is the radius of the scatterer, ρ is the density of the scatterer, ρ_w is the density of the fluid, Δx is the displacement of the scatterer from a state of equilibrium, l is the thread length, and g is free fall acceleration.

In a series of experiments performed on different days, we obtained the dependences of the radiation force acting on a target on the power at the source, which, according to the theory, should have a linear character (Fig. 6). In the experiments, the linear dependence was confirmed, but on different days, different slopes of the straight lines were obtained. This scatter can be explained mainly by in inaccuracy setting up the scatterer in the same region of the field for each replication of the experiment.

To increase the accuracy in measuring the force and repeatability of positioning the scatterer, an alternative scheme of fixing the scatterer was chosen (Fig. 4b). The sphere is not suspended but fixed on four elastic rubber threads. These threads are fastened to the scatterer on four sides. The entire system is set up in a rigid ring frame, the location of which in turn is assigned by a positioning system with micrometer screws with a positioning accuracy of 0.01 mm. In such a scheme, the sphericity of the scatterer is violated somewhat more than in the previous one, since the number of fixing points has increased. The fixation by four rubber threads also has a high sensitivity to small displace-

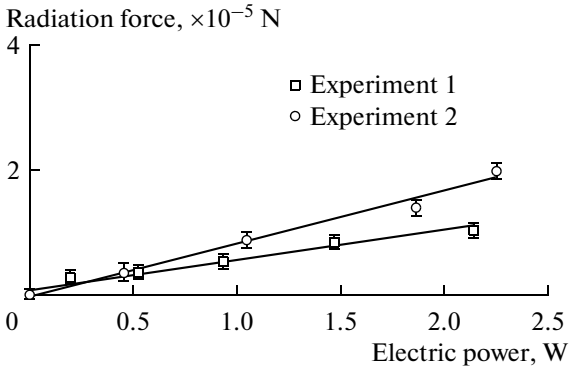

Fig. 6. Dependence of acoustic radiation force on electric power fed to acoustic transducer (displacement measured by laser). Experiments were conducted on different days. For plot with square experimental points, the coefficient of the straight line $k_1 = 0.483 \times 10^{-5}$ N/W; with circles, $k_2 = 0.828 \times 10^{-5}$ N/W.

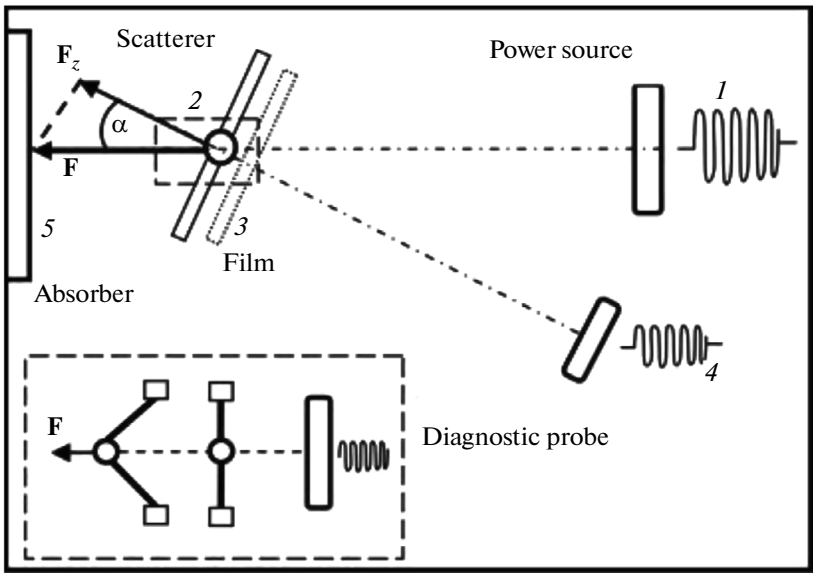

Fig. 7. Scheme of experimental setup with acoustic method of measuring displacement of scatterer. Acoustic power source *1* with resonance frequency $f = 1.119$ MHz, steel spherical scatterer *2*, sound-transparent film *3*, diagnostic probe *4* with operating frequency $f = 5$ MHz and absorber *5* to eliminate acoustic wave reverberations.

ments of the scatterer (when using sufficiently soft rubber threads). In addition, an advantage is the absence of displacement of the scatterer from the source axis under the action of the acoustic force. The elastic threads were chosen such that they introduced no distortions into the field structure, and the size of the ring frame was chosen larger that the beam diameter in the studied region. Thus, the choice of the type of suspension and determination of the optimal region of the field allow us to speak about the maximum closeness of the experimental conditions to those used in constructing the numerical model (a spherical scatterer in the field of a plane wave).

To increase accuracy, the method of measuring displacement was also changed in comparison to the conventional optical method. We used the principle of ultrasound echolocation (Fig. 7). A scatterer is placed in a water tank and attached in a ring frame by four elastic threads. The frame is rigidly fixed to a mechanical positioning system. At a distance of 325 mm from the center of the scatterer is the source of a power "pushing" beam radiating at a frequency of 1.199 MHz. At some angle to the scatterer at a distance of 195 mm from it is a diagnostic probe combined with an automatic positioning system (Velmex Unislide VP9000, United States) with step motors with a positioning accuracy along three axes of 2.5 μm and vertical rotation of 0.01 deg. The distance between the scatterer and the diagnostic probe was chosen such that the position of the diagnostic probe did not influence the structure of the forcing beam. The diagnostic probe was a plane broadband transducer with a diameter of 13 mm (Panametrics M109SM, Olympus Corp., Japan). To increase the signal reflected from the target, focusing was applied, which was ensured by an acoustic lens. Measurements were conducted as follows. A signal generator (HP 33120A) sent a short tone burst consisting of ten periods with a frequency of 5 MHz to the diagnostic transformer and an oscilloscope (Tektronix TDS 520A, United States) for control. A trigger pulse from another generator (Agilent 33250A) was fed to the oscilloscope, thereby ensuring the start of a power pulse in the required time interval and of the required duration. The delay time of the reflected diagnostic signal with deviation of the scatterer was measured by the oscilloscope. Thus, one operational cycle of the system consists of the following elements, depicted in Fig. 8. The cycles follow at a rate of 5 Hz, which corresponds to a cycle duration of 200 ms. From 190 ms, a pulse is emitted at a frequency of 1.119 MHz, exerting a powerful action on the scatterer. During the subsequent 300 μs, the diagnostic transducer operates, sending short sequential pulses and receiving corresponding echo signals (reflections from the sphere). Within several seconds of 5 Hz cycles, the scatterer is displaced from its state of equilibrium to a certain distance determined by the force of the action and the elasticity of the threads. Measurement of the arrival time of the reflected diagnostic pulses makes it possible to observe this displacement with a high accuracy.

The magnitude of the radiation force when the scatterer is fixed on elastic threads is determined by the known value of displacement in accordance with Hooke's law:

$$F_{\text{rad}} = -kd, \tag{12}$$

where k is the effective stiffness coefficient of all four threads and d is displacement. Here, the geometry of

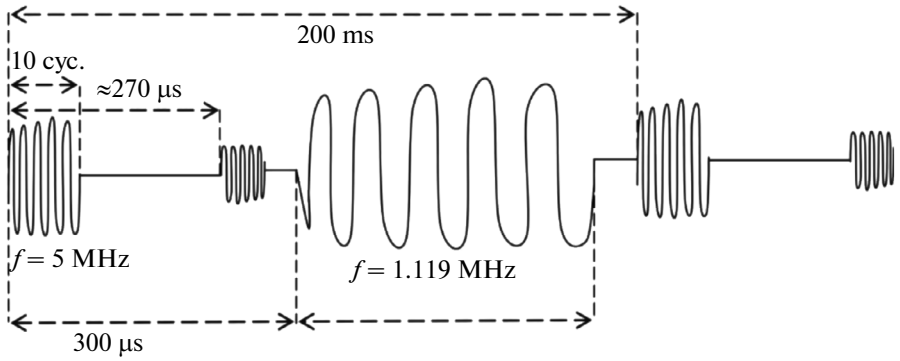

Fig. 8. One operating cycle of experimental setup to measure displacement by acoustic method. The diagnostic pulse consists of 10 periods; at a time delay of 270 μs from it, the pulse reflected from the scatterer is detected ; a power pulse consists of 212610 periods.

the experiment introduces a small correction to the value of the measured radiation force (Fig. 7). Since the diagnostic transducer is located at an angle α to the direction of wave propagation, the size of the displacement measured by it is proportional to some component of the radiation force acting on the sphere. In the general case, reconstruction of the real value of the radiation force can be quite a complex problem. However, in the case of plane wave, the radiation force acting on the scatterer is found from the relation $F = \frac{F_z}{\cos\alpha}$, where F_z is the force calculated by formula (12). Angle α in the experiment was found by photographing the setup from above and measuring the corresponding angle. It was $\alpha_1 = (33.0 \pm 0.5)°$ during the first experiment and $\alpha_2 = (36.5 \pm 0.5)°$ in the second experiment.

There are many different methods for determining the effective stiffness coefficient k. In the experiment an approach was chosen that was also based on the phenomenon of the radiation force and the principle of echolocation. When the scatterer is fixed on four elastic threads, it is an oscillatory system, the resonance frequency of which depends on the stiffness of the threads and the effective mass of the scatterer $\omega_0 = 2\pi f_0 = \sqrt{k/m}$. The effective mass of the scatter is added from the proper mass ($m_0 = (710 \pm 5)$ mg) and the associated mass arising as a result of fluid flow around the scatterer ($\Delta m = \frac{4}{3}\pi a^3 \frac{\rho_0}{2} = (46 \pm 5)$ mg). Thus, from the known values of the effective mass and rate of proper oscillations of the system, it is easy to calculate the effective stiffness of the threads.

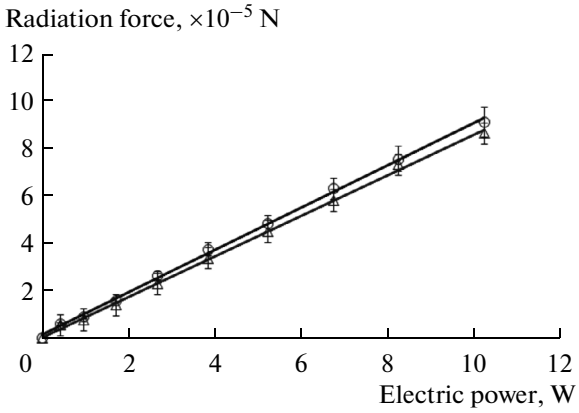

Fig. 9. Dependence of radiation force on electric power fed to transducer (displacement measured by echolocation). Experiments were conducted on different days. For the plot with triangular experimental points, the coefficient of the straight line $k_1 = 0.890 \times 10^{-5}$ N/W; with circles, $k_2 = 0.854 \times 10^{-5}$ N/W.

To generate oscillations of the system, pulse action was also used along with the radiation force. During such action, the system responds with oscillations at the resonance frequency. Displacements of the scatterer during oscillations is measured by the principle of echolocation with sound pulses, as described above. The resonance frequency of oscillations of the scatterer is determined by quadrature processing of the received signals, in which the main measured parameter is the signal phase, which slowly changes with time.

Experiments were conducted on different days to measure the radiation force and effective stiffness of the threads by the above-described methods (Fig. 10). It was found that the radiation force acting on the sphere for an electric power of $W \approx 11$ W corresponds to a displacement of the scatterer of $x \approx 0.3$ mm.

During measurements with the steel spherical scatterer attached by four elastic threads, the found effective stiffness coefficient $k = \omega_0^2 m = (0.215 \pm 0.007)$ kg/s^2. Here, both experiments confirmed the linear dependence of the radiation force on the total acoustic power (experimental points are approximated by a straight line with a reliability coefficient of approximation of $R^2 = 0.998$); the obtained relative measurement error is no more than 5–7%, in contrast to the 12–15% for suspension by two thin threads. Note also that the coefficient of the slope of the line obtained while measuring displacement of the scatterer by the acous-

tic method, as well as during suspension on four elastic threads, proved very close to the coefficient obtained when measuring the displacement of the scatterer on thin threads using the optical method.

CONCLUSIONS

The paper presents results of numerical simulation of the force action on metal spheres, conducted using a Fortran algorithm based on the classical solution to the problem of the acoustic radiation force exerted on an elastic spherical scatterer. It was shown that the dependences of the normalized value of the radiation force of the acoustic wave frequency agree well with similar plots for specific materials obtained earlier by other authors.

An experimental setup was implemented to determine the acoustic radiation force based on a method used by other authors, which consists in suspending a scatterer by a thin thread and measuring its displacement using a laser beam. It was shown that in the indicated method, the source of the error is related to measuring the position of the scatterer due to its nonaxial displacement when measuring the force.

A novel method is developed for high-precision measurement of the acoustic radiation force for a target in the form of solid spheres; the method is based on measuring the displacement of the receiver using echolocation by ultrasound pulses. An experimental setup was created for studying the force action of spherical targets of millimeter size using this method. In the experiments with steel spheres of millimeter size in water, a force measurement accuracy of 5 μN was achieved. As well, the theoretically predicted linear character of the dependence of the radiation force on the acoustic intensity was proved experimentally.

ACKNOWLEDGMENTS

The study was supported by a grant from the Russian Science Foundation (no. 14-15-00665).

REFERENCES

1. A. P. Sarvazyan, O. V. Rudenko, and W. L. Nyborg, Ultrasound Med. Biol. **36**, 1379 (2010).
2. I. N. Kanevskii, Sov. Phys. Acoust. **7**, 1 (1961).
3. G. G. Denisov, Acoust. Phys. **46**, 287 (2000).
4. B. I. Il'in and O. K. Eknadiosyants, Sov. Phys. Acoust. **14**, 452 (1969).
5. E. L. Gershenzon and O. K. Eknadiosyants, Sov. Phys. Acoust. **10**, 127 (1964).
6. O. V. Rudenko and S. I. Soluyan, Sov. Phys. Acost. **17**, 97 (1971).
7. S. D. Danilov and M. A. Mironov, Sov. Phys. Acoust. **30**, 280 (1984).
8. N. G. Semenova, Sov. Phys. Acoust. **20**, 65 (1974).
9. A. P. Gur'ev and N. G. Semenova, Sov. Phys. Acoust. **25**, 163 (1979).
10. A. Shaw and V. Hodnett, Ultrasonics **48**, 234 (2008).
11. A. Shah, J. D. Harper, B. W. Cunitz, Y. N. Wang, M. Paun, J. C. Simon, W. Lu, P. J. Kaczkowski, and M. R. Bailey, J. Urol, **187**, 739 (2012).
12. L. P. Gor'kov, Sov. Phys. Dokl. **6**, 772 (1962).
13. K. Yosioka and Y. Kawasima, Acustica, **5**, 167 (1955).
14. T. Hasegawa and K. Yosioka, J. Acous. Soc. Am. **46**, 1139 (1969).
15. V. N. Alekseev, Sov. Phys. Acoust. **29**, 77 (1983).
16. G. T. Silva, J. Acous. Soc. Am. **130**, 3541 (2011).
17. O. A. Sapozhnikov and M. R. Bailey, J. Acous. Soc. Am. **133**, 661 (2013).
18. A. A. Doinikov, J. Acous. Soc. Am. **96**, 3100 (1994).
19. T. Hasegawa, K. Yosioka, and A. Omura, Acustica, **22**, 145 (1969).
20. F. Dunn and A. J. Averbuch, Acustica **38**, 58 (1977).
21. T. F. W. Embleton, J. Acous. Soc. Am. **26**, 46 (1954).
22. S. Chen, G. T. Silva, R. Kinnick, J. Greenleaf, and M. Fatemi, Phys. Rev. E: Statist., Nonlin., Soft Matter Phys. **71**, 056618 (2005).
23. P. M. Morse and H. Feshbakh, *Methods of Theoretical Physics* (McGraw Hill, New York, 1953; InLit, Moscow, 1960), Vol. 2.
24. Cherkesov, L.B., *Hydrodynamics of Surface and Internal Waves* (Naukova Dumka, Kiev, 1976), [in Russian].
25. T. Hasegawa and T. Kido, C. W. Min, T. Iizuka, and C. Matsuoka, Acoust. Sci. Technol. **22**, 273 (2001).
26. O. A. Sapozhnikov, Yu. A. Pishchal'nikov, and A. V. Morozov, Acoust. Phys. **49**, 354 (2003).
27. O. A. Sapozhnikov, A. E. Ponomarev, and M. A. Smagin, Acoust. Phys. **52**, 324 (2006).
28. W. Kreider, P. V. Yuldashev, O. A. Sapozhnikov, N. Farr, A. Partanen, M. R. Bailey, and V. A. Khokhlova, IEEE Trans. Ultrason. Ferroelectr. Freq. Control **60**, 1683 (2013).

Translated by A. Carpenter